

Electrochemical Investigation of Interaction of *Candida albicans* with Titanium-Nickel Implant in Human Saliva

Bin Qiao¹, Tao Lv^{2*}

¹ College of Plant Protection, Northwest A&F University, Taicheng Road, Yangling District, Xianyang City, Shanxi Province 712100, P.R. China

² Guangzhou Medical University, GuangZhou, Guangdong 510182, P.R. China

*E-mail: taoluopursuit@sina.com

Received: 24 October 2021 / Accepted: 3 December 2021 / Published: 5 January 2022

Titanium and its alloys have been widely adopted in dental prosthetics due to their excellent biocompatibility, light weight, high resilience and good corrosion resistance. The human oral cavity is the second largest microbial host system after the human intestine, with a large number of microbial species. This complex environment of multiple groups of microorganisms promotes the formation of biofilms on the surface of oral implant titanium materials, leading to possible peri-implant inflammation which accelerates the surface corrosion of the titanium implant material. *Candida albicans* is a common fungus, and the study of the interaction between *Candida albicans* and titanium alloys is of great importance for the later systematic study of the corrosion effect of the fungus on the metal. In this study, fluorescence microscopy, scanning electron microscopy and electrochemical analysis techniques were adopted to systematically study the formation of microbial films of *Candida albicans* on the surface of titanium-nickel alloy. The electrochemical behavior of the corrosion of titanium-nickel alloy by *Candida albicans* were investigated with open circuit potential, potentiodynamic polarization curves and electrochemical impedance spectroscopy. The combined action of metabolites produced by *Candida albicans*, the extracellular polymer matrix and the formation of microbial film led to the changes in the corrosion electrochemistry of titanium-nickel alloy.

Keywords: Candiada albicans; Titanium alloy; Biofilm; Corrosion; Potentiodynamic polarization

1. INTRODUCTION

Due to its good corrosion resistance, strong mechanical properties and better biocompatibility, titanium and its alloys have been widely adopted in dentistry as hard tissue replacement materials such as dental implants, dental brackets, orthodontic wires and orthodontic materials [1–3]. Since titanium and its alloys have better performance than traditional natural materials, they are favored by doctors and patients. The strong corrosion resistance of titanium and its alloys results from the formation of a passivated TiO₂ film on its surface [4–7]. However, titanium and its alloys in the passivated state still

have a certain reactivity, which means that the dissolution and re-passivation of the passivated film are in a dynamic balance. As the external environment changes, the balance between the two is disrupted and the corrosion of titanium and its alloys is accelerated or inhibited, producing metal ions, which results in changes in the composition of saliva [8–11]. The excess V^{4+} , Al^{3+} , Ni^{2+} produced by dissolution have been proved to have toxic effects on humans. Among them, excess aluminum ions are believed to cause Alzheimer's disease, while nickel ions are associated with cytotoxic mouth. Therefore, the corrosion of titanium and its alloys in the oral environment is a problem that cannot be ignored [12–15]. It is of great importance to clarify the corrosion pattern and corrosion mechanism of titanium and its alloys in the oral environment and propose corresponding measures to avoid the toxic effects of metal ions on human body after the corrosion of titanium and its alloys [16–19].

However, the oral has an extremely complex environment. A normal human oral cavity contains up to 100-200 microbial species. Such a large number of microorganisms has become an essential factor that affect human health and limits the widespread use of titanium and its alloys in human oral cavity. The microorganisms contained in the oral cavity include bacteria, fungi, protozoa, mycoplasma and viruses [20–25], which are mutually constrained and interdependent, and they combined to maintain the balance of the microbial system inside the human oral cavity [26,27]. In addition, the presence of a large number of microorganisms inevitably has a corrosive effect on the implant materials. In the early days, the research on oral microbial corrosion mainly focused on the corrosion effect of bacteria on restorative materials [26,28–30]. However, as another important group of microorganisms, fungi account for more than 60% of the oral microbial species, thus the corrosion of oral restorative materials by fungi is a problem that cannot be ignored. *Candida spp.* is the most important type of fungi and presents in 25-50% of healthy human oral cavities, vaginas and digestive tracts. *Candida spp.* is a class of conditionally pathogenic microorganisms, which are harmless in most cases, but if some internal body functions change and the environment is conducive to their growth, they will multiply rapidly and grow mycelium to cause diseases [31–35], among which *Candida albicans* causes about 25-75% of cavity candidiasis that occur up to 90% in the elderly population. The major reason for the pathogenicity of *Candida albicans* is its excellent adhesion ability. *Candida albicans* can secrete glycoproteins that bind to glycoprotein receptors on the mucosal surface, allowing the cells to adhere to the mucosal surface. In addition, electrostatic gravitational force and hydrophobicity of its cells also promote the adhesion [36]. The formation of mycelium contributes to efficient nutrient uptake by *Candida albicans* and accelerates its proliferation, thus increasing its virulence and deteriorating the substrate environment [37–40].

In this work, the corrosion of titanium-nickel alloy in the presence of *Candida albicans* in a simulated oral saliva environment was investigated by comparing the corrosion morphology analysis and corrosion kinetics analysis to derive the effect of *Candida albicans* on the corrosion of titanium-nickel alloy.

2. EXPERIMENTAL

2.1 Titanium alloy and pre-treatment

The titanium-nickel alloy was purchased from Baoji Xinli Metal Materials Co., Ltd. and its composition is shown in Table 1.

Table 1. Composition of titanium nickel alloy.

Element	Ti	Ni	C	O	N	H	Other
Wt%	44.01	55.84	0.07	0.04	0.03	0.01	<0.001

The titanium-nickel alloy was cut into a volume of 2.0 cm × 2.0 cm × 0.1 cm specimens. Before the electrochemical test, the surfaces of the titanium-nickel alloy specimens were soldered with a copper wire of 20 cm in length, which was sealed in epoxy resin on the side connected to the alloy to make a working electrode (area of 4.0 cm²). Before the surface morphology test, a small hole was drilled in the middle of the surface of the titanium-nickel alloy specimens to facilitate the suspension of the alloy sample in the environment to be tested. All the titanium-nickel alloy specimens to be tested were polished with different grades of silicon carbide sandpaper on the working surface, and then cleaned three times with acetone, ethanol and distilled water, after which the titanium-nickel alloy specimens were immersed in 2.5% (v/v) glutaraldehyde solution and 75% (v/v) ethanol solution for 1 h and sterilized in the ultra-clean bench.

2.2 Preparation of culture media, artificial saliva and buffer solutions

Solid culture medium: glucose (10.0 g), peptone (10.0 g) and yeast powder (5.0 g) were weighed and dissolved in 950 mL of deionized water, and fixed into a 1000 mL volumetric flask. Afterwards, the solution was divided into 250 mL triangular flasks, and agar powder (1.5-2.0 g per 100 mL) was added. It was sterilized at 121°C under high temperature and high pressure for 20 min, and then was cooled down to solid medium.

Liquid culture medium: glucose (10.0 g), peptone (10.0 g) and yeast powder (5.0 g) were weighed and dissolved in 950 mL of deionized water, and fixed into 1000 mL volumetric flask. Afterwards, the solution was dispensed in triangular flasks, autoclaved at 121°C for 20 min, and cooled down as liquid culture medium.

The components of the artificial saliva are shown in Table 2. The pH of the artificial saliva was adjusted to 6.7 with 0.1 M HCl and it was autoclaved at 121°C for 20 min.

Table 2. Composition of artificial saliva.

Na ₂ HPO ₄	NaCl	KSCN	KH ₂ PO ₄	NaHCO ₃	KCl	Urea	Peptone	Glucose	Yeast
0.26	6.20	0.33	0.20	1.50	1.20	1.50	10.00	10.00	5.00
(g/L)									

PBS buffer solution: 4.26 g Na₂HPO₄, 24.00 g NaCl, 0.81g KH₂PO₄ and 0.60 g KCl were dissolved in 950 mL deionized water, and the pH was adjusted to 7.40 with 0.1 M HCl. Deionized water was added to a 1000 mL volumetric flask and sterilized at 121°C under high temperature and pressure for 20 min. It should be diluted 3 times with deionized water before being used.

2.3 Activation and growth curve determination of *Candida albicans*

0.3-0.4 mL of liquid culture medium was dropped into the anatomical tube and shaken gently to dissolve the lyophilized bacterium into suspension. 0.2 mL of the suspension was transplanted on the plate medium, after which the rest of the bacteria was added into the liquid culture medium, and incubated at 28 °C. The activated *Candida albicans* were stored in 30% glycerol and put into the refrigerator for subsequent experiments.

1.0 mL of activated *Candida albicans* solution was added into 100 mL of inactivated artificial saliva, shaken well and incubated in a constant temperature shaker at 37°C with a speed of 150 r/min. 3.0 mL of culture solution was taken into the cuvette every 2h, the wavelength of UV-vis spectrophotometer was adjusted to 530 nm, and the absorbance was measured. Dilution was carried out when the absorbance was greater than 1.5. The growth curve was measured three times in parallel, and then the growth curve was plotted with incubation time as the horizontal coordinate and absorbance as the axis.

2.4 Electrochemical behavior characterization

Candida albicans (1 mL mother liquor) was added to 150 mL of artificial saliva, and the group without microbial addition was used as the control group. The sterile titanium-nickel alloy working electrode was incubated in artificial saliva (28°C, 120 rpm/min) under anaerobic conditions for different times (24h, 120h and 240h), after which the open circuit potential (OCP), electrochemical impedance spectroscopy (EIS) and polarization curves of the alloy electrode at different incubation times were tested with an electrochemical workstation. The OCP test time was 1000 s, the EIS test frequency was 10^{-1} - 10^5 , and the excitation amplitude was 10 mV. The potentiodynamic polarization scan range was -1.5 V-2.0 V with a scan rate of 1 mV/s.

3. RESULTS AND DISCUSSION

The growth curve of the *Candida albicans* is shown in Figure 1. It can be clearly seen that *Candida albicans* went through four stages of typical microbial growth: sluggish phase, logarithmic growth phase, stable phase and declining phase [41,42]. In the initial stage of the experiment (0-20 h), *Candida albicans* grew slowly in the medium. After 20 h, the number of newborn microorganisms reached a certain balance with the number of dead microorganisms after the rapid multiplication of *Candida albicans* by secondary division. A stable period (58-80 h) appears in the growth curve. 120 h later, with the reduction of nutrients in the medium and the accumulation of metabolic waste, the growth of *Candida albicans* was no longer favored. The number of dead microorganisms exceeded the number of newborn microorganisms. The total number of microorganisms began to decline, and the growth of *Candida albicans* entered the declining phase. The measurement of microbial growth curve is beneficial to the selection of microorganisms with consistent growth status to ensure the reliability of experimental results [43]. In the experiment, microorganisms were selected at the end of the logarithmic growth phase

and the beginning of the stable phase, with more typical of the biological characteristics and metabolic activity of microorganisms. Figure 1 shows that the logarithmic growth phase of *Candida albicans* is 20-60 h, while the stable phase is 58-80 h. Therefore, *Candida albicans* was cultivated in medium for 48 h to achieve the best growth state, and transferred the bacterial solution to the reaction flask in the ultra-clean table for subsequent experiments.

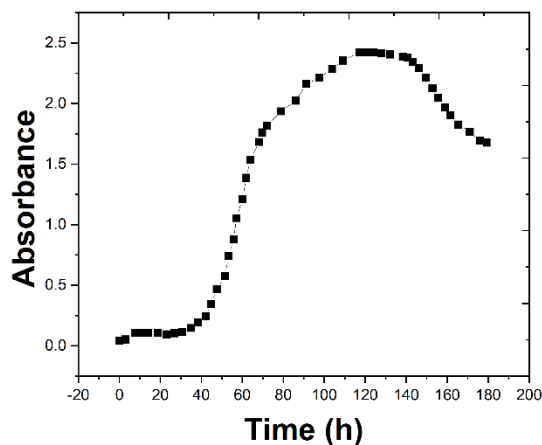


Figure 1. Growth curve of *Candida albicans*.

Figure 2 shows the pH test results of the solution medium in the presence and absence of *Candida albicans* growth. It can be found that the pH of the artificial saliva solution without *Candida albicans* was basically unchanged, with a value of about 9.30 and being alkaline, mainly for the reason of Maillard reaction between the sugars in the artificial saliva and the peptone to produce Schiff base. It is an imine alkaline compound, which makes the pH of the medium solution elevated. In addition, a small amount of urea in artificial saliva can also be decomposed under these conditions to form ammonia, which dissolves in water to raise the pH [44–46]. In contrast, the pH of the solution tends to decrease in the presence of *Candida albicans*, which indicates that the major metabolites of *Candida albicans* are acidic and can reduce the pH of the environmental solution. The strongest acid-producing effect of *Candida albicans* is at 48 h, which indicates that *Candida albicans* has the strongest vitality and the most vigorous metabolism at this time.

Figure 3 shows the fluorescence image of titanium-nickel alloy after 120 h immersion in artificial saliva containing *Candida albicans*. It can be found that *Candida albicans* exists in two biomorphs: oval or round yeast and striated or hyphae, which may be resulted from the production of population-sensing molecules. The formation of *Candida albicans* biofilm is associated with the growth rate of the fungus. As the immersion time increases, the growth of the fungus enters the logarithmic phase, the metabolism of *Candida albicans* is accelerated and the number of mycelium increases, becoming the main microbial form. The biofilm of *Candida albicans* is not a simple cell accumulation, but a three-dimensional structure with complex interlacing of mycelium and yeast, which is a highly structured microbial community [47], being conducive to the uptake of external nutrients and excretion of metabolic waste.

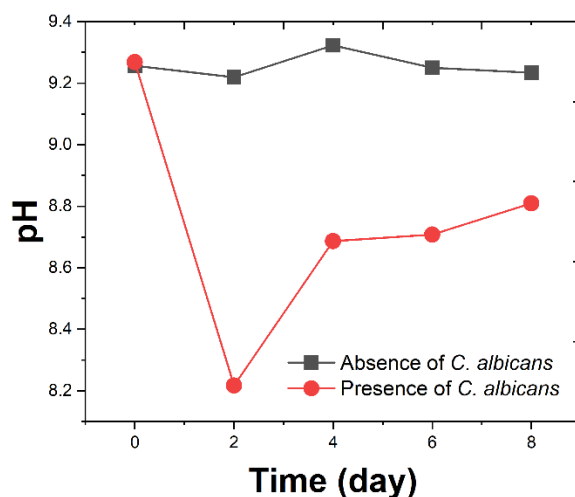


Figure 2. The pH of the artificial saliva solution medium with and without *Candida albicans*.

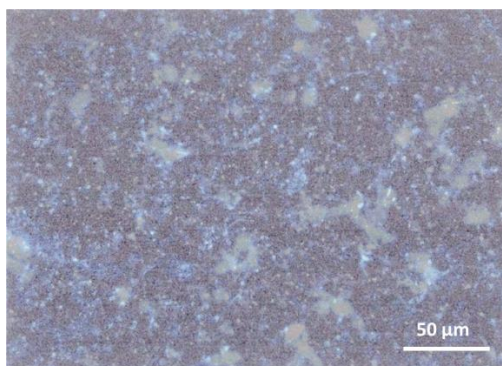


Figure 3. Fluorescence micrograph of titanium-nickel alloy surface in the presence of *Candida albicans*.

As shown in Figure 4, in the case of artificial saliva without *Candida albicans*, the OCP values of the titanium-nickel alloy first change negatively, reaching the most negative at 240 h, and then shift positively. After the addition of *Candida albicans*, the OCP values of titanium-nickel alloy show a significant fluctuation from positive to negative, indicating that the presence of *Candida albicans* leads to the pitting of titanium-nickel alloy [48]. Thus, the presence and absence of *Candida albicans* can cause different effects on titanium-nickel alloys immersed in artificial saliva. The formation of *Candida albicans* biofilm leads to the phenomenon of positive shift of OCP values.

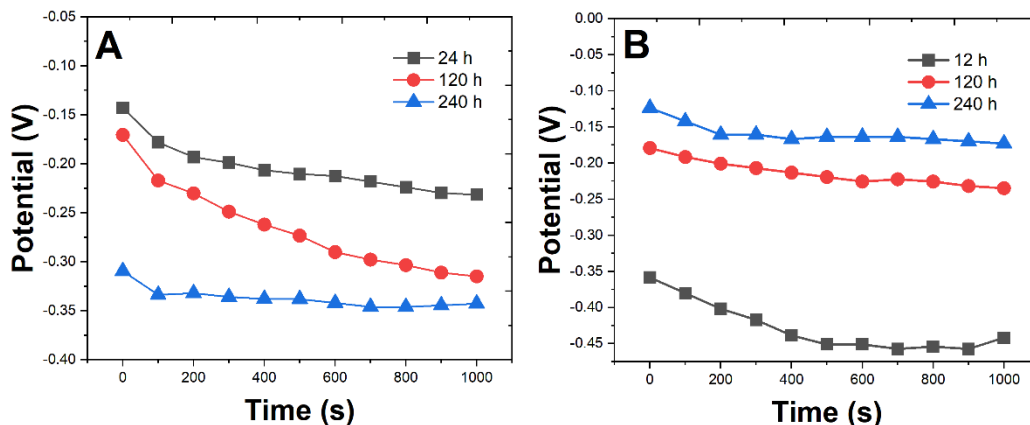


Figure 4. OCP variation curves of titanium-nickel in artificial saliva in the (A) absence and (B) presence of *Candida albicans*.

Figure 5 reveals that at the early stage of immersion, the potentiodynamic polarization curves show a strong passivation potential due to the presence of TiO₂ on the surface of titanium-nickel alloy. With the increase of soaking time, the passivation film was destroyed, the passivation effect was weakened and the corrosion rate of titanium-nickel alloy was accelerated [49,50]. From the comparison of the conditions with and without *Candida albicans*, it can be seen that the cathodic current of titanium-nickel alloy is slightly smaller in the presence of *Candida albicans* than that with the absence of *Candida albicans*.

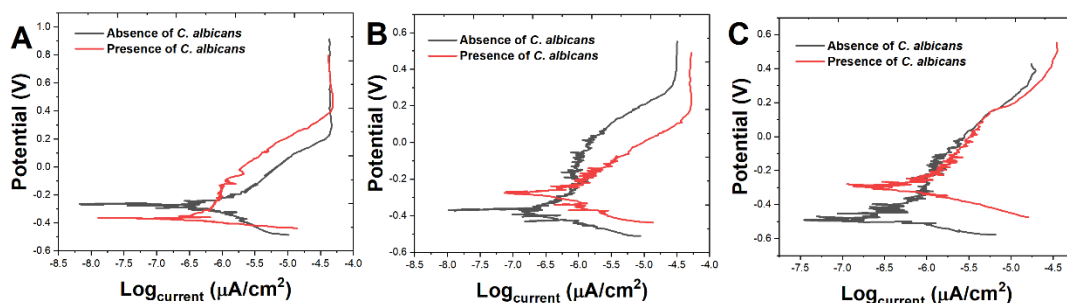


Figure 5. Potentiodynamic polarization curves of titanium-nickel alloy in artificial saliva with and without *Candida albicans* at (A) 24 h, (B) 120 h and (C) 240 h.

The anodic current is also smaller with the presence of *Candida albicans*, which indicates that the presence of *Candida albicans* at the early stage of immersion inhibited the corrosion rate of titanium-nickel alloy. 120 h later, the E_{corr} value began to shift positively in the presence of *Candida albicans*. With the increase of immersion time, the anode I_{corr} value increased continuously, indicating that the corrosion of titanium-nickel alloy was accelerated.

As presented in Table 3, E_{corr} shifts negatively from -0.244 V to -0.471 V with the increase of immersion time, and a slight positive shift of 0.166 V appears. In the *Candida albicans* solution, E_{corr} keeps shifting positively in fluctuations, which may be caused by the formation of microbial film on the

surface of titanium-nickel alloy. The fluctuation of E_{corr} indicates the pitting of titanium-nickel alloy in this system. In general, there is an overall increasing trend of E_{corr} when *Candida albicans* is contained. At 24 h, the I_{corr} in the *Candida albicans* state is smaller than that in the sterile state, indicating that the presence of *Candida albicans* inhibits the initial corrosion of titanium-nickel alloy. After 120 h, the bacterial state is larger than the sterile state, indicating that the presence of *Candida albicans* has the effect of accelerating the corrosion rate of titanium-nickel alloy [51].

Table 3. Fitted data on the kinetic potential polarization of titanium-nickel alloy in artificial saliva solution with and without *Candida albicans*.

Time (h)	Absence of <i>Candida albicans</i>				Presence of <i>Candida albicans</i>			
	E_{coor} (V)	$I_{\text{corr}} (\times 10^{-6} \text{ A/cm}^2)$	β_a (mV/decade)	β_c (mV/decade)	E_{coor} (V)	$I_{\text{corr}} (\times 10^{-6} \text{ A/cm}^2)$	β_a (mV/decade)	β_c (mV/decade)
24	-0.244	6.062	258	-230	-0.348	5.021	355	-43
120	-0.368	8.132	84	-102	-0.288	8.711	248	-21
240	-0.471	6.801	188	-122	-0.307	12.014	123	-144

As shown in Figure 6, the Nyquist plot is part of an imperfect semicircle with both the absence and presence of *Candida albicans*, indicating that the corrosion process of the titanium-nickel alloy is an electron transfer controlled process. The corrosion mechanism was not changed with the addition of *Candida albicans*. The magnitude of the axes of the plots shows that the titanium-nickel alloy has a strong corrosion resistance. After the addition of *Candida albicans*, the radius of Nyquist plot started to decrease after 120 h, and the transfer resistance decreased, indicating that *Candida albicans* can accelerate the dissolution corrosion rate of titanium-nickel alloy.

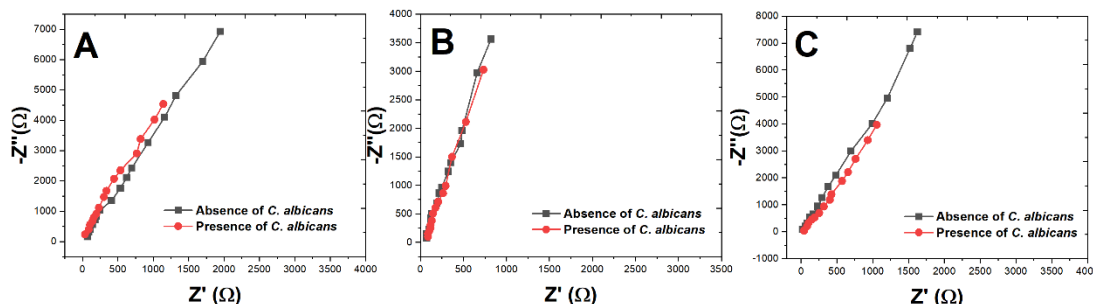


Figure 6. Nyquist plots of titanium-nickel in artificial saliva with and without *Candida albicans* at (A) 24 h, (B) 120 h and (C) 240 h.

Figure 7A-B reveals the surface morphology of titanium-nickel alloy with the absence and presence of *Candida albicans* at 120 h. It can be seen from the figures that *Candida albicans* adhered to the surface of the titanium nickel alloy uniformly and formed a biofilm. Figure 7C-D shows the surface morphology of the titanium-nickel alloy after the removal of biofilm. It is obvious that the surface corrosion of titanium nickel alloy after the removal of *Candida albicans* biofilm is more serious than

that of the no-microbial group, which indicates that the corrosion resistance of titanium nickel alloy is reduced with the presence of *Candida albicans*.

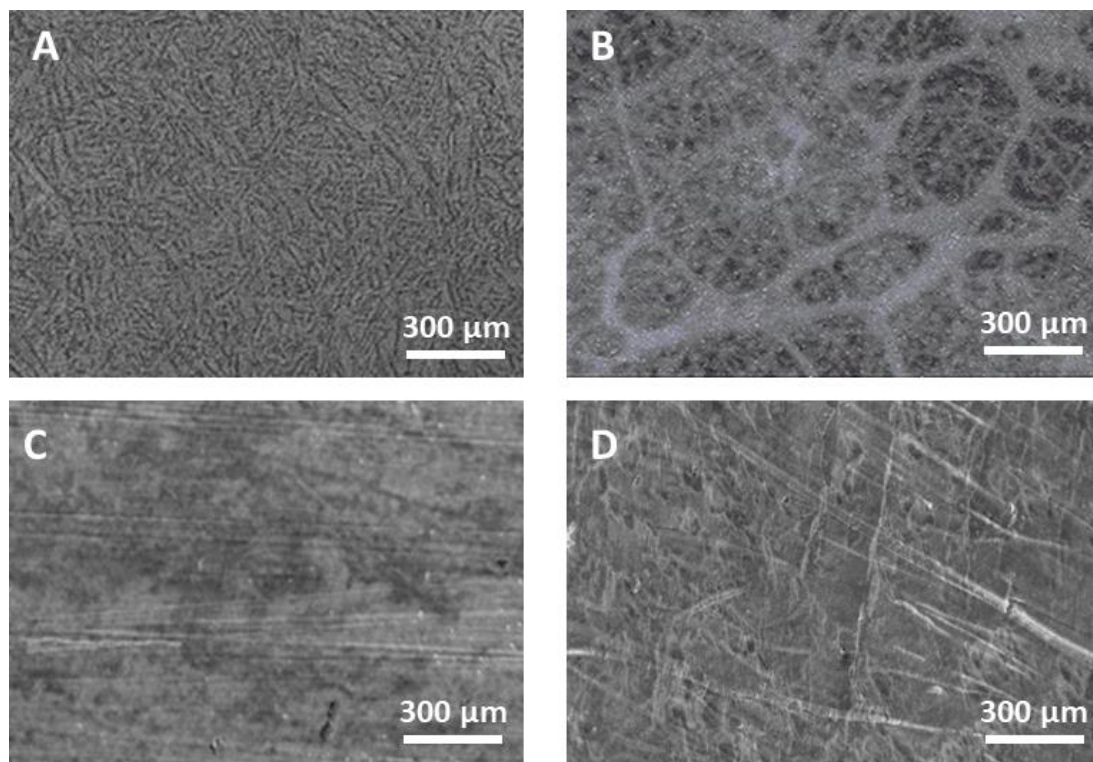


Figure 7. SEM images of titanium-nickel alloy surface in the (A) absence and (B) presence of *Candida albicans*. SEM image of titanium-nickel alloy surface (C) without *Candida albicans* and (D) removal of biofilm.

4. CONCLUSION

In conclusion, the formation of microbial films of *Candida albicans* on the surface of titanium-nickel alloy were systematically investigated in this study with fluorescence microscopy, scanning electron microscopy and electrochemical analysis techniques. The electrochemical behavior was examined via electrochemical methods such as open circuit potential, potentiodynamic polarization curves and electrochemical impedance spectroscopy. The combine action of metabolites produced by *Candida albicans*, the extracellular polymer matrix and the formation of microbial film can lead to the changes in the corrosion electrochemistry of titanium-nickel alloy. The results show a positive shift of E_{corr} , an increase of I_{corr} and a decrease of R_{ct} .

References

1. P.H. Le, D.H. Nguyen, A. Aburto-Medina, D.P. Linklater, R.J. Crawford, S. MacLaughlin, E.P. Ivanova, *ACS Appl. Bio Mater.*, 3 (2020) 8581–8591.
2. P.C. Passarelli, M. De Leonardis, G.B. Piccirillo, V. Desantis, R. Papa, E. Rella, G.N. Mastandrea Bonaviri, P. Papi, G. Pompa, G. Pasquantonio, *Antibiotics*, 9 (2020) 179.

3. L. Fu, K. Xie, A. Wang, F. Lyu, J. Ge, L. Zhang, H. Zhang, W. Su, Y.-L. Hou, C. Zhou, C. Wang, S. Ruan, *Anal. Chim. Acta*, 1081 (2019) 51–58.
4. J.G.S. Souza, M. Bertolini, A. Thompson, V.A.R. Barão, A. Dongari-Bagtzoglou, *Appl. Environ. Microbiol.*, 86 (2020) e02950-19.
5. D.M. Marques, V. de C. Oliveira, M.T. Souza, E.D. Zanotto, J.P.M. Issa, E. Watanabe, *Biofouling*, 36 (2020) 234–244.
6. R. Duan, X. Fang, D. Wang, *Front. Chem.*, 9 (2021) 361.
7. C. Li, F. Sun, *Front. Chem.*, 9 (2021) 409.
8. J. Zhou, Y. Zheng, J. Zhang, H. Karimi-Maleh, Y. Xu, Q. Zhou, L. Fu, W. Wu, *Anal. Lett.*, 53 (2020) 2517–2528.
9. L. Fu, W. Su, F. Chen, S. Zhao, H. Zhang, H. Karimi-Maleh, A. Yu, J. Yu, C.-T. Lin, *Bioelectrochemistry* (2021) 107829.
10. M. Mouhat, R. Moorehead, C. Murdoch, *Biomater. Investig. Dent.*, 7 (2020) 146–157.
11. S. D’Ercole, S. Di Lodovico, G. Iezzi, T.V. Pierfelice, E. D’Amico, A. Cipollina, A. Piattelli, L. Cellini, M. Petrini, *Biomedicines*, 9 (2021) 1261.
12. S.V. Agarwalla, K. Ellepola, N. Silikas, A.C. Neto, C.J. Seneviratne, V. Rosa, *Dent. Mater.*, 37 (2021) 370–377.
13. Y. Xu, Y. Lu, P. Zhang, Y. Wang, Y. Zheng, L. Fu, H. Zhang, C.-T. Lin, A. Yu, *Bioelectrochemistry*, 133 (2020) 107455.
14. B. Fan, Q. Wang, W. Wu, Q. Zhou, D. Li, Z. Xu, L. Fu, J. Zhu, H. Karimi-Maleh, C.-T. Lin, *Biosensors*, 11 (2021) 155.
15. H. Karimi-Maleh, Y. Orooji, F. Karimi, M. Alizadeh, M. Baghayeri, J. Rouhi, S. Tajik, H. Beitollahi, S. Agarwal, V.K. Gupta, *Biosens. Bioelectron.* (2021) 113252.
16. J. Li, S. Zhang, L. Zhang, Y. Zhang, H. Zhang, C. Zhang, X. Xuan, M. Wang, J. Zhang, Y. Yuan, *Front. Chem.*, 9 (2021) 339.
17. W. Li, W. Luo, M. Li, L. Chen, L. Chen, H. Guan, M. Yu, *Front. Chem.*, 9 (2021) 610.
18. H. Karimi-Maleh, M. Alizadeh, Y. Orooji, F. Karimi, M. Baghayeri, J. Rouhi, S. Tajik, H. Beitollahi, S. Agarwal, V.K. Gupta, S. Rajendran, S. Rostamnia, L. Fu, F. Saberi-Movahed, S. Malekmohammadi, *Ind. Eng. Chem. Res.*, 60 (2021) 816–823.
19. T.K. Pathak, R. Kroon, V. Craciun, M. Popa, M. Chifiriuc, H. Swart, *Heliyon*, 5 (2019) e01333.
20. H. Moradpoor, M. Safaei, A. Golshah, H.R. Mozaffari, R. Sharifi, M.M. Imani, M.S. Mobarakeh, *Inorg. Chem. Commun.*, 130 (2021) 108748.
21. P. Shende, B. Oza, R. Gaud, *Int. J. Polym. Mater. Polym. Biomater.*, 67 (2018) 1080–1086.
22. D. Achudhan, S. Vijayakumar, B. Malaikozhundan, M. Divya, M. Jothirajan, K. Subbian, Z.I. González-Sánchez, S. Mahboob, K.A. Al-Ghanim, B. Vaseeharan, *J. Environ. Chem. Eng.*, 8 (2020) 104521.
23. H. Karimi-Maleh, A. Ayati, R. Davoodi, B. Tanhaei, F. Karimi, S. Malekmohammadi, Y. Orooji, L. Fu, M. Sillanpää, *J. Clean. Prod.*, 291 (2021) 125880.
24. L. Fu, Y. Zheng, P. Zhang, J. Zhu, H. Zhang, L. Zhang, W. Su, *Electrochem. Commun.*, 92 (2018) 39–42.
25. M. Zhang, B. Pan, Y. Wang, X. Du, L. Fu, Y. Zheng, F. Chen, W. Wu, Q. Zhou, S. Ding, *ChemistrySelect*, 5 (2020) 5035–5040.
26. H. Karimi-Maleh, F. Karimi, L. Fu, A.L. Sanati, M. Alizadeh, C. Karaman, Y. Orooji, *J. Hazard. Mater.*, 423 (2022) 127058.
27. H. Karimi-Maleh, A. Khataee, F. Karimi, M. Baghayeri, L. Fu, J. Rouhi, C. Karaman, O. Karaman, R. Boukherroub, *Chemosphere* (2021) 132928.
28. J. Liu, T. Yang, J. Xu, Y. Sun, *Front. Chem.*, 9 (2021) 488.
29. Y. Zheng, Y. Huang, H. Shi, L. Fu, *Inorg. Nano-Met. Chem.*, 49 (2019) 277–282.
30. D. Montelongo-Jauregui, A. Srinivasan, A.K. Ramasubramanian, J.L. Lopez-Ribot, *J. Fungi*, 4 (2018) 66.

31. Y. Zheng, J. Zhu, L. Fu, Q. Liu, *Int J Electrochem Sci*, 15 (2020) 9622–9630.
32. L. Fu, Y. Zheng, P. Zhang, G. Lai, *Micromachines*, 12 (2021) 1048.
33. L. Palka, J. Mazurek-Popczyk, K. Arkusz, K. Baldy-Chudzik, *J. Oral Microbiol.*, 12 (2020) 1838164.
34. G. Darwish, S. Huang, K. Knoernschild, C. Sukotjo, S. Campbell, A.K. Bishal, V.A. Barão, C.D. Wu, C.G. Taukodis, B. Yang, *J. Prosthodont.*, 28 (2019) 1011–1017.
35. H. Karimi-Maleh, F. Karimi, S. Malekmohammadi, N. Zakariae, R. Esmaeili, S. Rostamnia, M.L. Yola, N. Atar, S. Movaghgharnezhad, S. Rajendran, A. Razmjou, Y. Orooji, S. Agarwal, V.K. Gupta, *J. Mol. Liq.*, 310 (2020) 113185.
36. S. Wei, X. Chen, X. Zhang, L. Chen, *Front. Chem.*, 9 (2021) 697.
37. S. Mina-Aponzá, S.P. Castro-Narváez, L.D. Caicedo-Bejarano, F. Bermeo-Acosta, *Molecules*, 26 (2021) 4813.
38. M. Cascione, V. De Matteis, P. Pellegrino, G. Albanese, M.L. De Giorgi, F. Paladini, M. Corsalini, R. Rinaldi, *Nanomaterials*, 11 (2021) 2027.
39. L. Fu, A. Wang, K. Xie, J. Zhu, F. Chen, H. Wang, H. Zhang, W. Su, Z. Wang, C. Zhou, S. Ruan, *Sens. Actuators B Chem.*, 304 (2020) 127390.
40. X. Zhang, R. Yang, Z. Li, M. Zhang, Q. Wang, Y. Xu, L. Fu, J. Du, Y. Zheng, J. Zhu, *Rev. Mex. Ing. Quím.*, 19 (2020) 281–291.
41. S. Sagadevan, S. Vennila, L. Muthukrishnan, B. Murugan, J.A. Lett, M. Shahid, I. Fatimah, O. Akbarzadeh, F. Mohammad, M.R. Johan, *Optik*, 224 (2020) 165515.
42. Y. Yue, L. Su, M. Hao, W. Li, L. Zeng, S. Yan, *Front. Chem.*, 9 (2021) 479.
43. E. Tambone, A. Marchetti, C. Ceresa, F. Piccoli, A. Anesi, G. Nollo, I. Caola, M. Bosetti, L. Fracchia, P. Ghensi, *Polymers*, 13 (2021) 2420.
44. S. Chen, J.K. Tsoi, P.C. Tsang, Y.-J. Park, H.-J. Song, J.P. Matinlinna, *Regen. Biomater.*, 7 (2020) 213–220.
45. H. Karimi-Maleh, Y. Orooji, A. Ayati, S. Qanbari, B. Tanhaei, F. Karimi, M. Alizadeh, J. Rouhi, L. Fu, M. Sillanpää, *J. Mol. Liq.*, (2020) 115062.
46. Z. Xu, M. Peng, Z. Zhang, H. Zeng, R. Shi, X. Ma, L. Wang, B. Liao, *Front. Chem.*, 9 (2021) 683.
47. O. Pazarci, U. Tutar, S. Kilinc, *Eurasian J. Med.*, 51 (2019) 128.
48. O.I. Timaeva, I.P. Chihacheva, G.M. Kuzmicheva, L.V. Saf'yanova, R.G. Chumakov, R.P. Terekhova, *Appl. Nanosci.*, 8 (2018) 1729–1741.
49. A.L. Rangel, C. Falentin-Daudré, B.N.A. da Silva Pimentel, C.E. Vergani, V. Migonney, A.P.A. Claro, *Surf. Coat. Technol.*, 383 (2020) 125226.
50. H. Owada, H. Narusawa, Y. Kataoka, T. Miyazaki, *Showa Univ. J. Med. Sci.*, 31 (2019) 159–166.
51. G.H. Waly, *Future Dent. J.*, 4 (2018) 8–15.